# Numerical analysis of pressures on rigid structures using the smoothed particle hydrodynamics method

**M. Sunara, B. Gotovac, J. Radnić, and A. Harapin***

*Faculty of Civil Engineering, Architecture and Geodesy, University of Split, Matice Hrvatske 15, Split, Croatia.*

**Abstract.** This study aims to carry out a numerical analysis of hydrodynamic pressures on rigid structures caused by dynamic base excitation. First, the model for fluid simulation is presented based on a numerical approach called Smoothed Particle Hydrodynamics (SPH) method. Then, the described model is used to measure the pressure exerted on rigid structures. In the performed analysis, the structures of different geometries (a rectangular tank with vertical sides, rectangular tanks with one inclined side of constant slope, and a cylindrical tank) are exposed to simple harmonic horizontal base excitations. The obtained hydrodynamic pressures on the sides of the tanks are compared with analytical and other numerical solutions.

## 1. Introduction

Structures, such as dams, water tanks (reservoirs), offshore structures, pipelines, water towers, etc., which are in direct contact with fluid, are often applicable to engineering practices, and the fluid pressures on these structures are regarded as a significant factor in their designing. The total pressures on the structure under earthquakes can highly increase, or fall below, the water vapor pressure and produce a phenomenon known as cavitation. Such extreme pressures can cause significant damage to and destruction of structures. A number of factors can affect the distribution of pressures: compressibility of the fluid, geometry of the system, stiffness of the structure, type of dynamic load,

etc. To estimate the level of structural safety reliably, precise determination of total pressure on the structure is of importance.

The first rigorous hydrodynamic analysis of the dam-reservoir system was carried out by Westergaard [1] in 1933. In his novel study, he considered an infinitely long reservoir with incompressible fluid and derived an analytical expression to distribute the hydrodynamic pressures exerted on a rigid dam during a horizontal harmonic ground motion. Westergaard's expression has been then applied in design standards until today. Two decades later, Zangar [2] experimentally obtained the distribution of hydrodynamic pressures of incompressible water on an inclined barrier using the electrical analogy method. Housner developed a mechanical analogue model [3] which is one of the oldest and most widely used tools for explaining the fundamentals of fluid dynamics in rectangular and cylindrical liquid storage tanks subjected to horizontal ground motions. In the following decades, extensive analyses were performed by a number of researchers, one of the most distinguished and cited of whom

*. *Corresponding author. Tel.: +385 21 303 358*
*E-mail addresses: marina.sunara@gradst.hr (M. Sunara);*
*blaz.gotovac@gradst.hr (B. Gotovac); jure.radnic@gradst.hr*
*(J. Radnić); harapin@gradst.hr (A. Harapin)*

was Chopra [4], who suggested analytical expressions for the hydrodynamic response of dam-reservoirs and evaluated the compressibility effects during harmonic and arbitrary ground motions. Chwang [5] proposed several solutions for hydrodynamic pressures on inclined dam faces with horizontal and inclined reservoir bottoms. All of the mentioned analyses were performed based on the assumption that water level would not change during earthquakes, which was valid only for small ground displacement and/or quite fast excitation. Chwang [6] was the first to include the rise of free surface and nonlinear convective acceleration and took into account a rigid vertical wall and constant ground acceleration. According to all of the abovementioned studies (and many others), the hydrodynamic pressures play a key role in the behavior of a dam-reservoir-foundation system.

Although Fluid-Structure Interaction (FSI) approach has recently become the focus of scientific research, investigation of forces caused by the liquid pressure on rigid structures is still of interest. In a number of cases, displacements of a structure are quite small which is indicative of the rigidity of the structure; therefore, the full FSI approach is not necessary, thus saving time and money during the analysis. Recently, a number of studies in the literature on the hydrodynamic pressures on rigid structures have been conducted using different water modeling approaches. Seghir et al. [7] studied the coupling numerical model of boundary and finite elements suitable for the dynamic dam-reservoir interaction. Chen and Yuan [8] developed a finite-difference method to analyze the pressures on arc dams during earthquakes, which incorporated the free-surface waves and nonlinear convective acceleration. Lefrançois et al. [9] studied the seismic safety of concrete gravity water intake structures of typical hydroelectric facilities. Valamanesh et al. [10] incorporated the Endurance Time (ET) method in the seismic analysis of concrete gravity dams. Hariri-Ardebili and Kianoush [11] considered the hydrodynamic pressure effect inside the opened joints in a dam during a seismic action using the heuristic approach. Ferdousi et al. [12] studied the behavior of arch dams under earthquake and further investigated the effects of foundation discontinuities, proper boundary conditions, etc. [13].

A significant phenomenon with considerable influence on the response of the fluid containers/accumulations during an earthquake, especially when it is coincident with the natural frequencies of the free-liquid surface, is sloshing. Since it can drastically change the pressures on the fluid, many researchers have measured such effects. Tyvand and Miloh [14] studied the incompressible impulsive sloshing in open containers. Lee et al. [15] evaluated the sloshing resistance performance of an Liquefied Natural Gas (LNG) carrier insulation system. Fonfach et al. [16]

compared the results of numerical sloshing simulations and those of the Lagrangian and lumped mass models and many others as well.

In this paper, distribution of hydrodynamic and total pressures on rigid structures exposed to dynamic base excitations was investigated through a 3D numerical model based on the Smoothed Particle Hydrodynamic (SPH) method. Detailed validation of the original numerical model through similar physical processes (creation of waves by landslides, dam-break propagation over wet beds, and wave-structure interaction) can be found in [17], i.e., a study that compared the obtained numerical results with the well-known analytical results and provided some examples of rigid structures exposed to dynamic base excitation where use of the SPH method would bring about several advantages. The main objective of the present study was to determine the accuracy of the SPH method, which, as an essentially integral method, could describe the real pressure in a discrete point on the rigid structure. In this paper, the pressure correction on the boundaries of the fluid domain was also presented. In addition, such improvement can provide more reliable data on the hydrodynamic pressures on the structure, which can be of importance in conducting numerical simulations of FSI. Recently, many authors have performed several experimental and numerical investigations for further improvement of the developed numerical model [18,19].

## 2. Numerical model

### 2.1. Fluid governing equations

Fluid flow is caused by the action of externally applied forces such as gravity, shear, rotation, pressure differences, etc. The fluid flows may be classified as either inviscid or viscous. Inviscid flows are frictionless flows characterized by zero viscosity. No real flows are inviscid, but there are numerous fluids and flow situations in which viscous effects can be neglected. Inviscid flows may be further classified as either compressible or incompressible, depending on whether the density variations are large or relatively negligible. In this study, the fluid is considered as laminar viscous and weakly compressible.

The Navier-Stokes equations represent a set of equations that describe the motion of fluid substances such as liquids and gases [20,21]:

$$\rho\frac{\partial v_i}{\partial t} = \rho R_i - \nabla p + \mu \nabla^2 v_i, \tag{1}$$

where, $v_i$ is the vector of velocity, $\rho$ the mass-density, $p$ the pressure, $\mu$ the viscosity of the fluid, and $R_i$ the sum of external forces acting on the fluid. The Navier-Stokes equations are regarded as a base point for all fluid movement simulations. For complex situations

involving cavitation, turbulence, aerodynamics, hydro-
dynamics etc., the solutions to the Navier-Stokes equa-
tions can be exclusively provided by numerical models.

### 2.2. Smoothed Particle Hydrodynamics (SPH)

SPH is a Meshfree Particle Method (MPM) developed
to simulate the astrophysics problems. It was first pro-
posed by Lucy [22] and Gingold and Monaghan [23] and
was widely applied to all kinds of engineering problems
of continuum solid and fluid mechanics. Nowadays,
this method is popularly used for simulating the free
surface flows. This method is described in such papers
as Monaghan [24,25]. This study presents only a brief
description of this method.

The MPMs generally refer to a class of meshfree
methods that employ a set of finite number discrete
particles to record the movement of a system and
represent the state of it. Each particle is usually
associated with some physical characteristic related
to a specific problem (mass, energy, position, density,
pressure, etc.) and represents a part of the continuum
domain. The particles range from a macro (a very large
astronomical scale) to micro (atomic) scale. Depending
on the used mathematical model, the MPMs can be
either deterministic or probabilistic. The deterministic
MPMs directly employ the used governing system
equation of physical law. In the deterministic MPMs,
once the initial and boundary conditions are given,
the particle evolution in the later time stages can be
theoretically and precisely determined based on the
physical laws that define the problem. Although the
probabilistic MPMs also utilize the governing system
equation of physical law, their approach is based on
statistical principles. The SPH method has mixed
features. It was initially developed as a probabilistic
method, yet later modified and applied as a determin-
istic MPM.

The fundamental principle of the SPH method
is to approximate any function $A(\vec{r})$ with a unique,
uniform, smooth, and compact kernel function $W(\vec{r} -
\vec{r}', h)$ that is defined all over the space $\Omega$, with the
smoothing length $h$:

$$A(\vec{r}) = \int_{\Omega} A(\vec{r}')W(\vec{r} - \vec{r}', h)\, d\vec{r}, \qquad (2)$$

where $r$ is any point in $\Omega$, $r'$ a neighboring point, and
$h$ the smoothing length or core radius. Smoothing
length is a scaling factor that controls the smoothness
or roughness of the kernel. This integral representation
in discrete notation leads to the approximation of the
function $A(\vec{r}_a)$ at a particle of interest (particle "$a$"):

$$A(\vec{r}_a) = \sum_b m_b \frac{A_b}{\rho_b} W(\vec{r}_b - \vec{r}_a, h), \qquad (3)$$

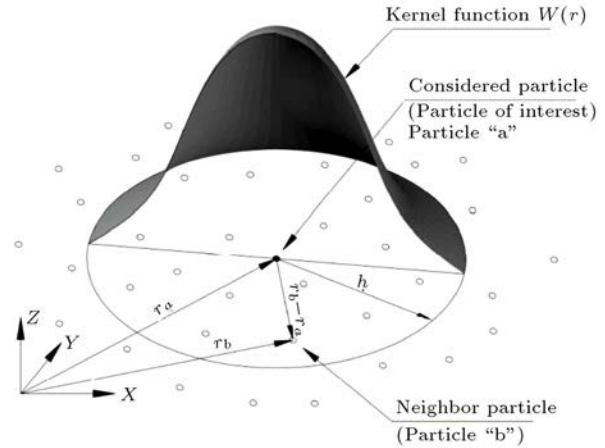where the summation is, overall, the neighboring



**Figure 1.** Particle approximation in the Smoothed
Particle Hydrodynamics (SPH) method.

particles "$b$" within the region of the kernel function
(Figure 1). The mass and density are denoted by $m_b$
and $\rho_b$, respectively, and $W$ is the kernel function.

The kernel function should satisfy several condi-
tions such as positivity, compact support, and normal-
ization. It should also be monotonically decreasing
with the increasing distance from the particle and
behave like a delta function as the smoothing length
tends to zero. One of the most often used kernel
functions is the cubic spline [20,21] defined by:

$$W(\vec{r}_b - \vec{r}_a, h) = \frac{1}{\pi h^3} \begin{cases} 1 - \frac{3}{4}q^2 + \frac{3}{4}q^3 & 0 \le q \le 1 \\ \frac{1}{4}(2 - q)^3 & 1 \le q \le 2 \\ 0 & q \ge 2 \end{cases} \qquad (4)$$

which was also employed in this study, with $q = r/h$.
Obviously, the obtained results significantly depend on
the choice of the kernel function [20].

One of the governing equations of fluid dynamics
is the momentum conservation equation, which, in SPH
form, is [20,21]:

$$\frac{\partial \vec{v}}{\partial t} = \sum_b m_b \left( \frac{P_b}{\rho_b^2} + \frac{P_a}{\rho_a^2} + \Pi_{ab} \right) \vec{\nabla} W_{ab} + \vec{g}, \qquad (5)$$

where $g$ is the gravitational acceleration; $P_a$, $\rho_a$, $P_b$,
$\rho_b$ are the pressures and densities corresponding to
particles $a$ and $b$; $\Pi_{ab}$ is the viscosity term proposed
by Monaghan [24]:

$$\Pi_{ab} = \begin{cases} \frac{-\alpha \bar{c}_{ab} \mu_{ab}}{\bar{\rho}_{ab}} & \vec{v}_{ab} \cdot \vec{r}_{ab} < 0 \\ 0 & \vec{v}_{ab} \cdot \vec{r}_{ab} > 0 \end{cases} \qquad (6)$$

where $\mu_{ab} = h\vec{v}_{ab}\vec{r}_{ab}/(\vec{r}_{ab}^2 + \eta^2)$, $\eta^2 = 0.01h^2$, $\bar{c}_{ab} =
(c_a + c_b)/2$, $\vec{r}_{ab} = \vec{r}_a - \vec{r}_b$, and $\vec{v}_{ab} = \vec{v}_a - \vec{v}_b$. In
addition, $c_a$, $c_b$, $\vec{r}_a$, $\vec{r}_b$, $\vec{v}_a$, $\vec{v}_b$ are the speed of sound,
position, and velocity corresponding to the particle $a$
or $b$, respectively. Moreover, $\alpha$ is a free parameter

that can change according to the problem ($\alpha = 0.1$ for water).

The SPH method assumes that the masses and mass-densities for all particles are known before the method starts. While the particle mass is a user-defined constant, the mass-density is a continuous field of the fluid, which must be computed [20,21].

Changes in the fluid density are calculated through the continuity equation:

$$\frac{\partial \rho}{\partial t} = \sum_b m_b \vec{v}_{ab} \vec{\nabla} W_{ab}. \tag{7}$$

In SPH formalism, the fluid is treated as weakly compressible; thus, the fluid pressure can be obtained by the equation of state. In this paper, Tait's equation is used for the equation of state:

$$P = \frac{c_0^2 \rho_0}{\gamma} \left[ \left( \frac{\rho}{\rho_0} \right)^7 - 1 \right], \tag{8}$$

where $\rho_0$ is the reference density ($\rho_0 = 1000$ kgm$^{-3}$ for water) and $c_0$ is the speed of sound at reference density. Pressure is directly coupled to density through the equation of state. One of the disadvantages of this approach is that the pressure field of the particles has large oscillations. One of the solutions to overcoming this problem is density correction, i.e., re-assigning a density to each particle in every time steps. In this study, the Moving Least Squares (MLS) approach [26] was taken into account. Then, the new density is defined by:

$$\rho_a^{\text{new}} = \sum_b \rho_b W_{ab}^{MLS} \frac{m_b}{\rho_b} = \sum_b m_b \, W_{ab}^{MLS}. \tag{9}$$

The kernel can be corrected as shown in the following:

$$W_{ab}^{MLS} = W_b^{MLS}(\vec{r}_a) = \beta(\vec{r}_a) \cdot (\vec{r}_a - \vec{r}_b) W_{ab}, \tag{10}$$

where the correction vector $\beta$ is defined by:

$$\beta(\vec{r}_a) = A^{-1} \begin{bmatrix} 1 \\ 0 \\ 0 \\ 0 \end{bmatrix} \text{ where } A = \sum_b W_b(\vec{r}_a) \tilde{A} V_b, \tag{11}$$

where in matrix $\tilde{A}$ (shown in Box I), $x_a$, $y_a$, and $z_a$

represent the coordinates of point "a" and $x_b$, $y_b$, and $z_b$ represent the coordinates of point "b".

In this study, the previously described density correction algorithm was applied every 30 time steps. This correction could significantly improve the pressure distributions, especially those in the vicinity of the solid boundaries.

Furthermore, the fluid should satisfy the energy conservation equation:

$$\frac{\partial e_a}{\partial t} = \frac{1}{2} \sum_b m_b \left( \frac{P_b}{\rho_b^2} + \frac{P_a}{\rho_a^2} + \Psi_{ab} \right) \vec{v}_{ab} \vec{\nabla} W_{ab}, \tag{13}$$

where $\Psi_{ab}$ is the viscosity term.

The standard predictor-corrector scheme was adopted as the solver algorithm [20,21]. The time-step control involves the Courant-Friedrichs-Lewy (CFL) condition, force terms, and viscous diffusion term [27]. A variable time step is calculated according to [24]:

$$\Delta t = 0.3 \min(\Delta t_f, \Delta t_{cv}),$$

$$\Delta t_f = \min \left( \sqrt{h/|f_a|} \right),$$

$$\Delta t_{cv} = \min \frac{h}{c_s + \max \left| \frac{h \vec{v}_{ab} \vec{r}_{ab}}{\vec{r}_{ab}^2} \right|}, \tag{14}$$

where $\Delta t_f$ is based on the force per unit mass $|f_a|$, and $\Delta t_{cv}$ combines the Courant with viscous time step controls.

The boundary of the fluid domain, which represents tank geometry in this research, can described by a set of so-called dynamic boundary particles [20–29]. These boundary particles are forced to satisfy the same equations as the fluid particles, except they do not move according to the forces exerted on them and remain fixed in their position.

### 2.3. Pressures on the boundaries

Despite the employed pressure correction approach, Eqs. (9)–(12), pressures on the edges can still be very irregular and highly dependent on the geometry and load mainly due to the fact that the fluid at the edges is truncated. These (incorrect) pressures do not have a great influence on fluid movements [16,24,25], but on the forces on the structure. Although many corrections have been proposed to solve this problem (for example

$$\tilde{A} = \begin{bmatrix} 1 & (x_a - x_b) & (y_a - y_b) & (z_a - z_b) \\ (x_a - x_b) & (x_a - x_b)^2 & (x_a - x_b)(y_a - y_b) & (x_a - x_b)(z_a - z_b) \\ (y_a - y_b) & (x_a - x_b)(y_a - y_b) & (y_a - y_b)^2 & (y_a - y_b)(z_a - z_b) \\ (z_a - z_b) & (x_a - x_b)(z_a - z_b) & (y_a - y_b)(z_a - z_b) & (z_a - z_b)^2 \end{bmatrix}. \tag{12}$$

Box I

[28–30]), this problem is still the focus of interest to many researchers.

The present study proposed a new pressure correction on the edge of fluid domain. After calculating the pressures at the dynamic boundary particles [28], these pressures are averaged through the next expression:

$$P_a = \frac{\sum\limits_b \frac{P_b}{\vec{r}_b - \vec{r}_a}}{\sum\limits_b \frac{1}{\vec{r}_b - \vec{r}_a}}, \tag{15}$$

where $a$ denotes the particle of interest on the boundary (unmovable) and $b$ represents the fluid particle placed on the distance smaller than the core radius from particle $a$. The averaged fluid pressures fit the expected (analytical) values much better, which is very important for the determination of fluid forces on structure.

## 2.4. Note about model and software

The original SPH model/software was taken from [31] and upgraded with an arbitrary domain shape and an arbitrary type of external excitation. The original model was inspired from the significant works of Lucy (1977) [22] as well as Gingold and Monaghan (1977) [23] and was developed to a mighty engineering tool to simulate different phenomena in fluid such as viscosity and turbulence [21], surface tension [32], wave breaking [33], sloshing [34], sliding objects, wave impact on a structure, and so on. Further, the classical SPH formulation is particularly well suited for problems involving large fluid deformation and fluid continuity breaking that occur in highly nonlinear and potentially violent free surface flows [28].

The influence of boundary conditions, multiphase modeling, violent wave breakings, floating bodies, and interaction between the fluid and moveable/flexible structure are still among the open issues to be fully discovered in the SPH methods [34] that point to the limitations of this model.

## 3. Numerical tests

Several numerical tests of tanks with different structural geometries were performed using the previously described model. In all these tests, the structure of the tanks was assumed to be rigid and filled to a certain level with water. Then, it was exposed to simple harmonic horizontal base excitations. Additional hydrodynamic and total (hydrostatic + hydrodynamic) pressures on the side of the tank perpendicular to the direction of the excitation were also observed. Small-scale tanks were utilized in all performed numerical tests, thus expecting the obtained results and given conclusions to be indirectly applicable to the full-scale tanks during corresponding excitation.

## 3.1. Pressures on the vertical side of a rectangular tank

The distribution of hydrodynamic and total water pressures on the vertical side of a rigid rectangular tank is also analyzed. The tank dimensions were 3.0 m × 1.0 m × 1.5 m and the water level in the tank was 1.0 m (Figure 2). The tank was exposed to a simple harmonic ground acceleration $a$, with maximum acceleration $a_0$ and period $T_p$ (Figure 3).

The initial spatial distribution of particles and initial (hydrostatic) pressures of particles are shown in Figure 4. A relatively fine discretization was adopted. The initial spacing of particles was 0.05 m, and they were organized in a Cartesian grid. The total number of particles, including the boundary particles, was 38170.

### 3.1.1. Westergaard's hydrodynamic pressures
Westergaard derived an analytical solution for the distribution of hydrodynamic pressures $p_d$ exerted on a rigid dam during a horizontal harmonic ground motion, with the following assumptions taken into account [1]:
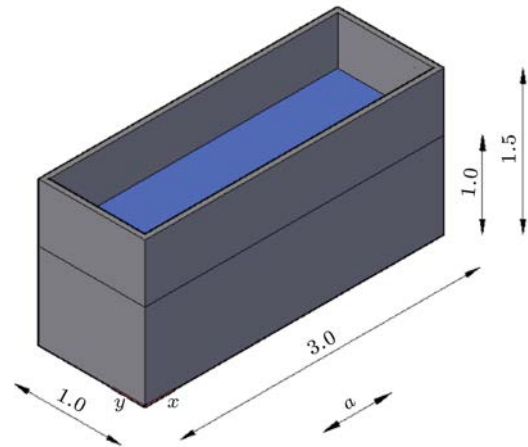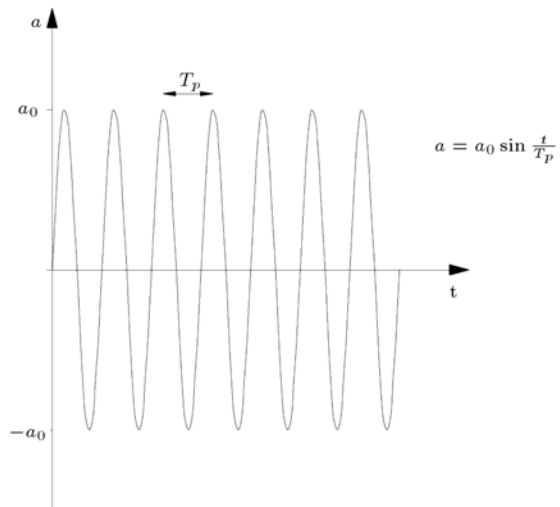


**Figure 2.** Tank geometry.


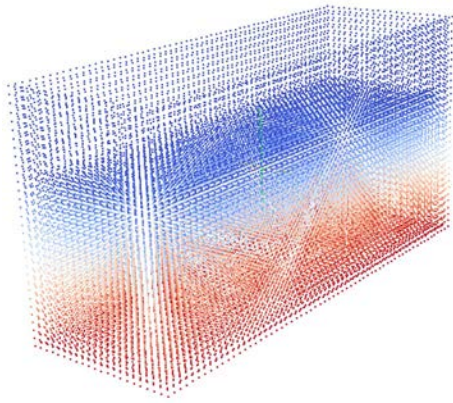
**Figure 3.** Adopted ground acceleration $a$.

**Figure 4.** Initial distribution of particles.

- The reservoir is infinitely long;
- The dam is rigid and infinitely wide;
- The dam has a vertical upstream face;
- The effects of waves on the free surface of water are negligible;
- The fluid is inviscid and incompressible.

His simplified analytical solution was given using the following approximate expression:

$$p_d = \frac{7}{8}\rho a_0 \sqrt{h(h-y)}, \tag{16}$$

where $\rho$ is the water density, $h$ the water level in the tank, and $y$ the water depth measured from the free surface. Housner solution [3] for elongated tanks coincides with Westergaard's.

According to Eq. (16), the solution was not dependent on the period of excitation, but only on the maximum acceleration of a simple ground motion. Obviously, Westergaard's solution can be defined as the oscillation of fluid particles around an equilibrium position. In this respect, his analytical solution is valid only when the period of excitation is longer than the fundamental resonance period for water pressure [4], but is shorter than the period that can cause big disturbances in water particles. The fundamental resonance period for water pressure can be calculated by:

$$T_1 = \frac{4h}{c_p}, \tag{17}$$

where $h$ is the water depth and $c_p$ is the speed of sound in water (1430 m/s). According to Eq. (17), the fundamental resonance period for water pressure of the analyzed system is 0.00279 s.

### 3.1.2. Hydrodynamic and total pressures with the SPH method

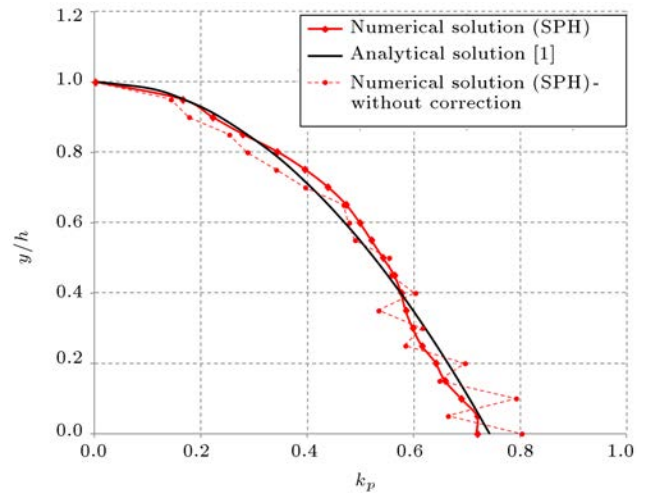Several tests with different periods of base excitations were performed, among which two of the most extreme



**Figure 5.** Hydrodynamic pressure coefficient $k_p$ on the right side of the tank at $T_p = 0.03$ s.

ones were studied. In all analyses, the maximum acceleration was assumed to be 0.5 g. In the first test, the period of excitation $T_p$ was 0.03 s, approximately 10 times longer than the fundamental resonance period for water pressure. The resonance should be avoided. Moreover, the applied excitation did not cause significant particle movements and consequently, the results of hydrodynamic pressures obtained by the SPH method could be compared with Westergaard's analytical solution [1]. The distribution of the maximum hydrodynamic pressures on the vertical side of the tank perpendicular to the direction of excitation is shown in Figure 5. The hydrodynamic pressure coefficient $k_p$ is defined by:

$$k_p = \frac{p_d}{\rho a_0 h}. \tag{18}$$

Apart from the visual comparisons given in Figure 5, the Root Mean Square (RMS) error was used to measure the differences between the analytical and numerical values, which was 0.0411 without additional correction of the pressures. By using the correction of the pressures, given in Eq. (15), the RMS error between the analytical and numerical results was measured as 0.02. Total pressures in the water, at specific times, for the harmonic ground acceleration for $T_p = 0.03$ s are shown in Figure 6. The expansion of the pressure wave in the water is visualized in Paraview [35], and the fluid surface remains calm.

The numerical results for hydrodynamic pressures obtained with the model based on the SPH method were in good agreement with the Westergaard's analytical solution for the period of excitation $T_p = 0.03$ s. However, slight inaccuracies between the numerical and analytical solutions are evident in Figure 5. Although no significant displacement of particles was observed in this period, the particles were still oscillating around
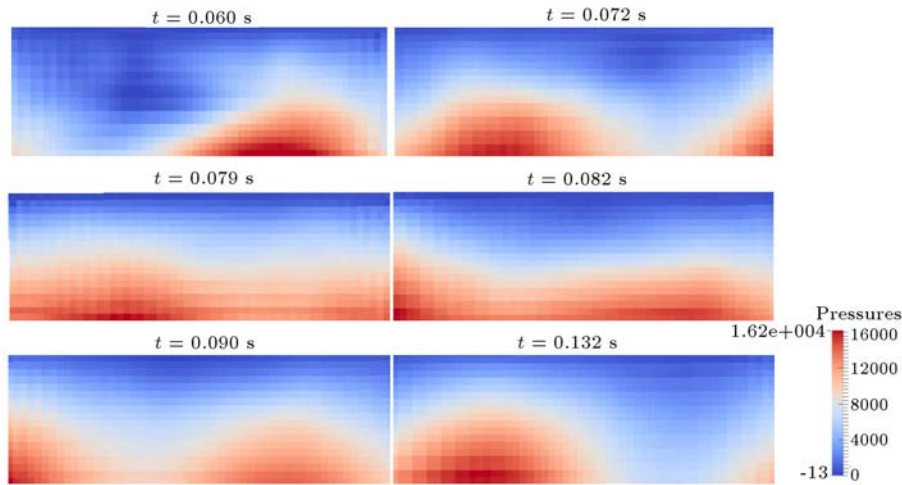
**Figure 6.** Expansion of the pressure (Pa) wave in the water for the harmonic ground acceleration at $T_p = 0.03$ s.

their equilibrium position, thus changing the density. According to Eq. (8), small changes in density causes large pressure changes, thus justifying these inaccuracies. Moreover, these inaccuracies are partially the result of different assumptions between the analytical and numerical solutions. In this numerical analysis, while a tank with finite dimensions was adopted, the analytical solution was valid for an infinitely long and wide reservoir.

In the second test, the period of excitation $T_p$ was 1.0 s, which was much longer than the fundamental resonance period for water pressure, yet shorter than the sloshing resonance period, which was around 2.0 s [4]. In this case, the fluid particles made notable waves on the fluid surface, the water level climbed up on the sides of the tank, and pressures increased. Obviously, the assumption of negligible waves on the free surface of water was not valid. The distribution of total pressures (hydrostatic and hydrodynamic) at some times on the sides of the tank for $T_p = 1.0$ s is shown in Figure 7.

It can be concluded that during the harmonic ground acceleration with a significantly longer period than the fundamental resonance period for water pressure, big churning and splattering with level rising of the water surface, could occur (Figure 8) which made changes in the pressures on the rigid barrier.

### 3.2. Pressures on the inclined side of a 3D tank

The distribution of hydrodynamic and total pressures generated by water on the inclined side of a rigid tank was analyzed in this study. The dimensions of the tank are the same as those shown in Section 3.1 (the rectangular tank), with only the right side of the tank inclined with a constant slope (Figure 9). Three constant slopes on the right side of the tank $\beta$ were taken into consideration: 15°, 30°, and 45°. The initial
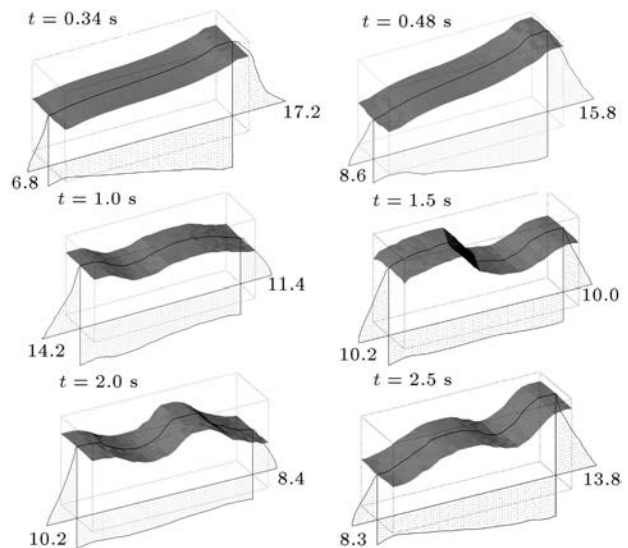


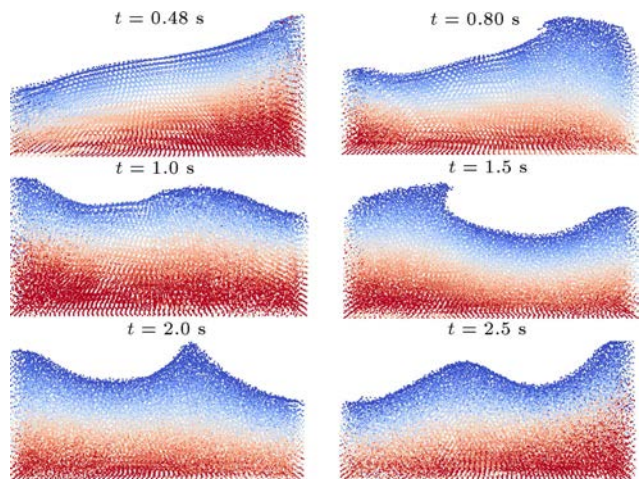**Figure 7.** Distributions of total pressures (kPa) at some times on the sides of the tank at $T_p = 1.0$ s.



**Figure 8.** Total pressures and sloshing in the water for the harmonic ground acceleration at $T_p = 1.0$ s.
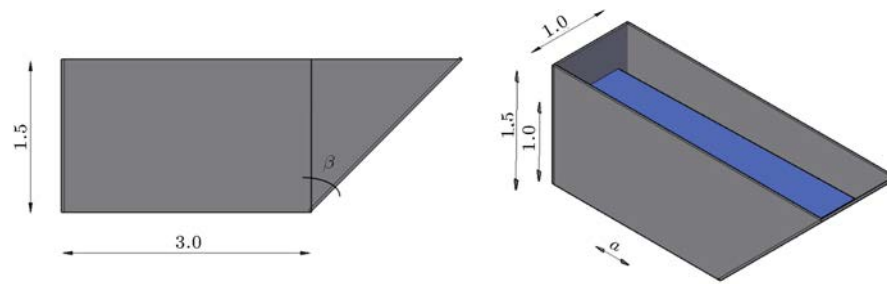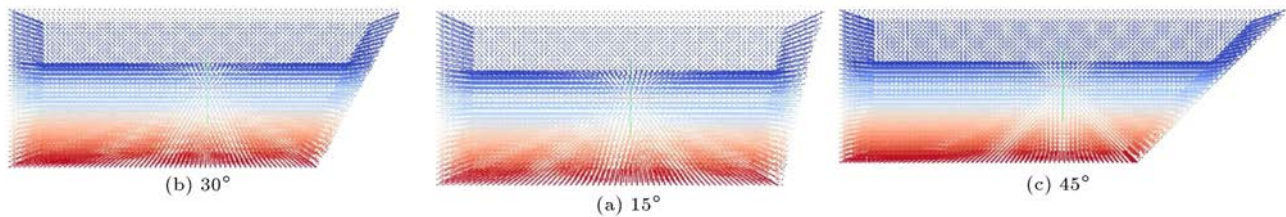
**Figure 9.** Tank geometry.



**Figure 10.** Initial distributions of particles for different slopes on the right side of the tank.

distributions of particles are shown in Figure 10. The initial spacing of particles organized in a Cartesian grid is 0.05 m. The tanks are exposed to simple harmonic horizontal base excitations with two different periods of oscillations $T_p$ (Figure 3). In all tests, the maximum acceleration was assumed to be 0.5 g. In the case of $\beta = 0°$, the pressure distribution is equivalent to the example in Section 3.1.

### 3.2.1. Analytical solution for hydrodynamic pressures
Chwang provided the exact solution for the fluid hydrodynamic pressure distribution during an earthquake on a rigid dam with the inclined upstream face of constant slope using the boundary integration method. His assumptions were very similar to Westergaard's. He considered the reservoir to be infinitely long and wide with an incompressible and inviscid fluid. The pressure distribution on the upstream face of the sloped dam is defined by:

$$p_d = \rho a_0 h k_p, \tag{19}$$

where the pressure coefficient $k_p$ is graphically presented in Figure 11 [5].

### 3.2.2. Hydrodynamic and total pressures with the SPH method
The distribution of pressures along the inclined side of the tank for horizontal harmonic base excitation with periods $T_p = 0.03$ s and $T_p = 1.0$ s, which are longer than the fundamental resonance period for water pressure [4], is analyzed. In all the tests, maximum acceleration of 0.5 g is assumed. Numerical results for hydrodynamic pressures obtained using the model based on the SPH method for $T_p = 0.03$ s are shown in Figure 12. The hydrodynamics pressure coefficient $k_p$ is defined by Eq. (18).
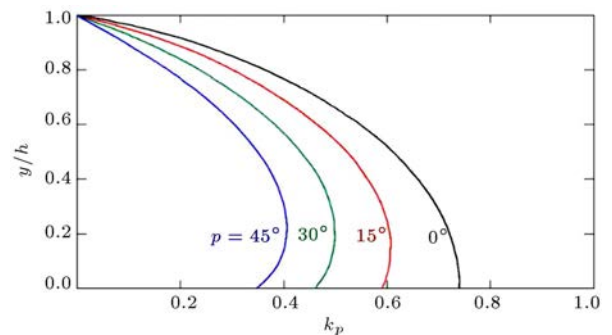


**Figure 11.** Pressure coefficient [5].

The numerical results are in relatively good agreement with the analytical solution [5] for the period of excitation $T_p = 0.03$, where such an excitation does not cause significant movements of particles. However, it can be noted that the discrepancies are slightly higher for the tank with a vertical wall and are increasing with the slope $\beta$. This can be explained by the uneven particle distribution on the sloping walls, causing even larger disturbances in density as a consequence of geometry.

The distributions of total pressures (hydrostatic and hydrodynamic) at some times on the sides of the tank for the tank with $\beta = 45°$ and $T_p = 1.0$ s are shown in Figure 13. In this excitation period, fluid particles make significant waves on the fluid surface, similar to the tests in Section 3.1. Thus, the assumption that the effects of waves on the free surface of water are negligible is not valid.

### 3.3. Pressures on a cylindrical tank
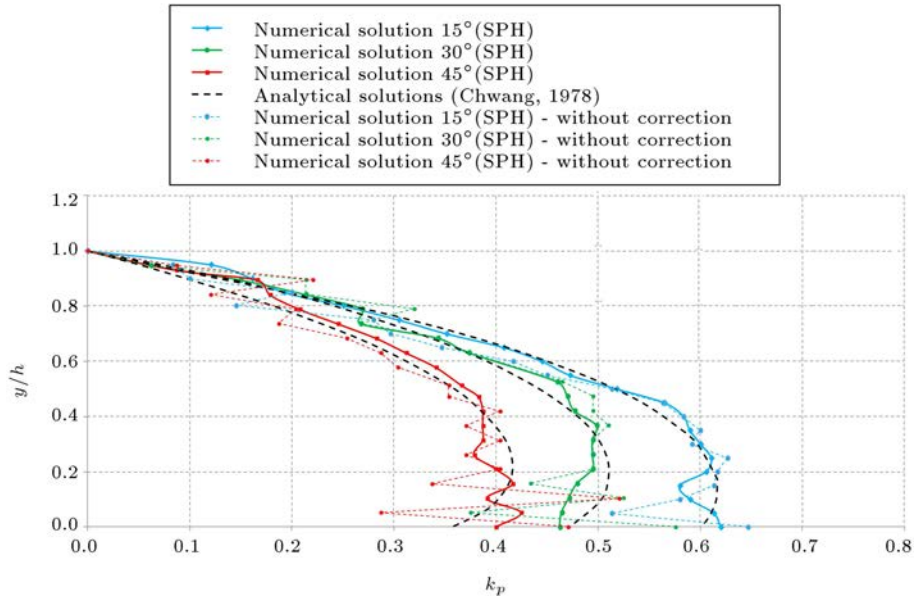The distribution of hydrodynamic and total pressures generated by water on a rigid cylindrical tank is ana-

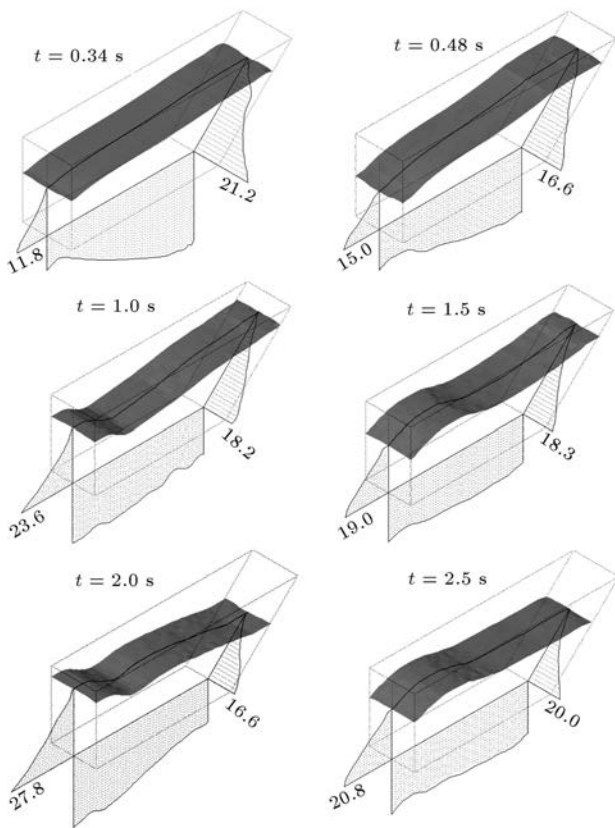**Figure 12.** Hydrodynamic pressure coefficient $k_p$ on the inclined side of the tank at $T_p = 0.03$ s.



**Figure 13.** Distributions of total pressures (kPa) at some times on the sides of the tank for $\beta = 45°$ at $T_p = 1.0$ s.



**Figure 14.** Tank geometry.



**Figure 15.** Initial distribution of particles.

lyzed (Figure 14). The diameter and height of the tank are 2.0 m and 1.0 m, respectively, with the water level in the tank being 0.6 m. The tank is exposed to simple horizontal harmonic ground accelerations according to
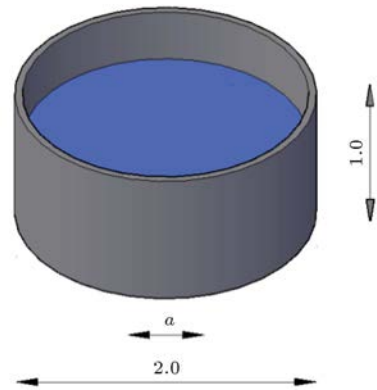
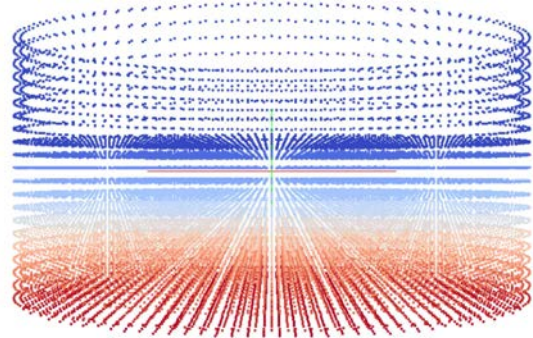Figure 3. The initial distribution of particles is given in Figure 15.

*3.3.1. Analytical solution for hydrodynamic pressures*
Using the Ritz variational method, Petrov and Moiseevd [36] derived an analytical solution for the distri-
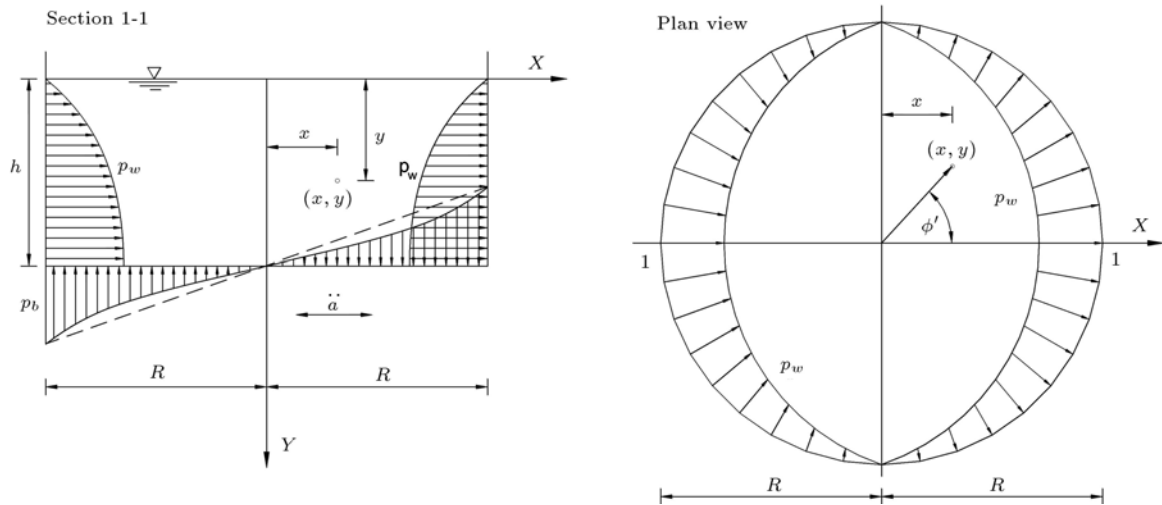
**Figure 16.** Hydrodynamic pressures on a cylindrical tank.

bution of hydrodynamic pressures on a rigid cylindrical tank exposed to a horizontal harmonic excitation (Figure 16). They assumed an inviscid incompressible liquid in a partially filled cylindrical tank. The analytical solution [36,37] for the distribution of hydrodynamic pressures is given by Eqs. (20) and (21), with the variables defined in Figure 16:

$$p_w = \rho_w \ddot{a}_0 h \left[ \sqrt{3} \cos \phi' \left( \left( \frac{y}{h} \right) - \frac{1}{2} \left( \frac{y}{h} \right)^2 \right) th \left( \sqrt{3} \frac{R}{h} \right) \right], \quad (20)$$

$$p_b = \rho_w \ddot{a}_0 h \left[ \frac{\sqrt{3}}{2} \cos \phi' \frac{sh \left( \sqrt{3} \frac{r}{h} \right)}{ch \left( \sqrt{3} \frac{R}{h} \right)} \right] ; \begin{bmatrix} 0 \leq r \leq R \\ 0 \leq \phi' \leq 2\pi \\ 0 \leq y \leq h \end{bmatrix} . \quad (21)$$

### 3.3.2. Hydrodynamic and total pressures with the SPH method

The distribution of pressures on the sides of the tank for horizontal harmonic base excitation in periods $T_p = 0.02$ s and $T_p = 0.7$ s is analyzed. These periods are longer than the fundamental resonance period for water pressure, which is 0.00167 s for the analyzed system. In all the conducted tests, maximum acceleration of 0.5 g is assumed.

When $T_p$ is 0.02 s, the excitation does not cause any significant particle movements and, consequently, the results of hydrodynamic pressures obtained by the SPH method can be compared with the analytical solution [36,37]. The distribution of the maximum hydrodynamic pressures on the right side of the cylindrical tank on the $xz$-plane at $T_p = 0.02$ s is shown in Figure 17. An estimated RMS error between the analytical results and the numerical results obtained by Finite Element Method (FEM) is 0.1871 kPa, and RMS error between the analytical results and the numerical results obtained by the SPH is 0.1271 kPa. It is evident that the obtained results are in relatively good
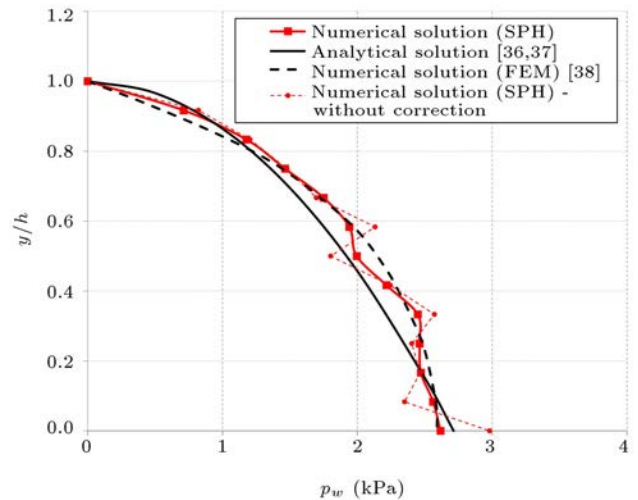


**Figure 17.** Distribution of hydrodynamic pressures [kPa] on the right side of the tank at $T_p = 0.02$ s.

agreement with the analytical results [36,37] and even better with the numerical results obtained with the FEM analysis [38]. The initial distribution of particles, in which each particle occupies equal volume, in the case of a cylindrical tank is even more irregular and, thus, inaccuracies are expected to occur.

The distributions of total pressures (hydrostatic and hydrodynamic) at some times on the sides of the tank at $T_p = 0.7$ s are shown in Figure 18. Similar to the rectangular tank, this excitation period, which is much longer than the fundamental resonance period for water pressure, causes significant churning and splattering with the water level rising on the borders and total pressures as a function of these effects.

### 4. Conclusion

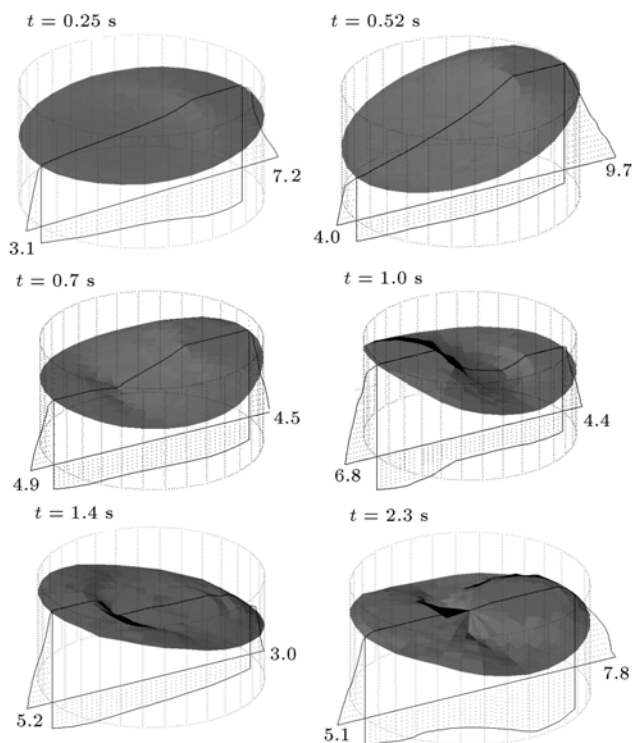The Smoothed Particle Hydrodynamics (SPH) method

**Figure 18.** Distribution of total pressures (kPa) at some times on the sides of the tank at $T_p = 0.7$ s.

is a Lagrangian meshless particle method, in which the problem domain was described by a finite number of moving particles. Each particle contained the physical determinants of a part of the volume such as mass, density, pressure, position, and velocity. Lately, the SPH method has rapidly developed and become a powerful tool for solving the fluid dynamics problems and fluid-structure interaction problems. It could employ various disciplines of science and industry.

In this study, the distribution of pressures (hydrodynamic and total) on rigid structures caused by horizontal ground excitations was investigated using a 3D numerical model based on the SPH method. Further, the main objective of this study was to determine the accuracy of the SPH method which, as an essentially integral method, could measure the real pressure on a rigid structure, easily compared with the well-known analytical expressions.

In the present analysis, rigid structures of various geometries filled with water (a three-dimensional tank with vertical sides, tanks with one inclined side of constant slope, and a cylindrical tank) were exposed to simple horizontal harmonic motions. The obtained results were compared with analytical and other numerical solutions. In case the excitation periods did not cause significant movements of particles, the obtained results of hydrodynamic pressures were in good agreement with the analytical solutions. On the contrary, in case the periods of excitation caused significant

waves in water, the analytical solution failed and only the numerical solution was provided. Therefore, the SPH method was suitable for distributing pressures on rigid structures when base excitations caused a significant change to the free surface. Based on the results presented in this paper, although the individual results deviated from the expected values, the integral method could describe the subject matter quite well.

These results can be applied to fluid-structure numerical simulation tests in which accurate hydrostatic and hydrodynamic pressures are employed as structure load.

## References

1. Westergaard, H.M. "Water pressures on dams during earthquakes", *Transactions, American Society of Civil Engineers* (ASCE), **98**(1835), pp. 418–433 (1933).

2. Zangar, C.N. "Hydrodynamic pressure on dams during to horizontal earthquakes", *Proc. Soc Experimental Stress Analysis*, **10**, pp. 93–102 (1953).

3. Housner, G.W. "Dynamic pressures on accelerated fluid containers", *Bulletin of the Seismological Society of America*, **47**(1), pp. 15–35 (1957).

4. Chopra, A.K., *Hydrodynamic Pressures on Dams During Earthquakes*, Department of Civil Engineering, University of California, Berkeley, Report No. 66–2, pp. 1–14 (1966).

5. Chwang, A.T. "Hydrodynamic pressures on sloping dams during earthquakes: Part 2, exact theory", *Journal of Fluid Mechanics*, **87**(2), pp. 342–348 (1978).

6. Chwang, A.T. "Nonlinear hydrodynamic pressure on an accelerating plate", *The Physics of Fluids*, **26**(2), pp. 383–387 (1983).

7. Seghir, A., Tahacourt, A., and Bonnet, G. "Coupling FEM and symmetric BEM for dynamic interaction of dam-reservoir systems", *Engineering Analysis with Boundary Elements*, Elsevier, **33**, pp. 1201–1210 (2009).

8. Chen, B. and Yuan, Y. "Hydrodynamic pressures on arch dam during earthquakes", *Journal of Hydraulic Engineering*, **137**(1), pp. 34–44 (2011).

9. Lefrançois, A., Léger, P., and Bouaanani, N. "Finite element seismic safety assessment of water intake structures", *Finite elements in analysis and design*, **83**, pp. 1–9 (2014).

10. Valamanesh, V., Estekanchi, H.E., Vafai, A., et al. "Application of the endurance time method in seismic analysis of concrete gravity dams", *Scientia Iranica, A.*, **18**(3), pp. 326–337 (2011).

11. Hariri-Ardebili, M.A. and Kianoush, M.K. "Seismic analysis of a coupled dam-reservoir-foundation system considering pressure effects at opened joints", *Structure and Infrastructure Engineering*, **11**, pp. 833–850 (2015).

12. Ferdousi, A., Gharabaghi, M.A.R., Ahmadi, M.T., et al. "Earthquake analysis of arch dams including the effects of foundation discontinuities and proper boundary conditions", *Journal of Theoretical and Applied Mechanics*, **52**(3), pp. 579–594 (2014).

13. Ahmadi, M.T. and Haghani, M. "Methods for design of large dam gates under seismic hydrodynamic action", *Proceedings of the U.S.-Iran Seismic Workshop*, pp. 18–20 (2012).

14. Tyvand, P.A. and Miloh, T. "Incompressible impulsive sloshing", *Journal of Fluid Mechanics*, **708**, pp. 279–302 (2012).

15. Lee, C.S., Cho, J.R., Kim, W.S., et al. "Evaluation of sloshing resistance performance for LNG carrier insulation system based on fluid-structure interaction analysis", *International Journal of Naval Architecture and Ocean Engineering*, **5**, pp. 1–20 (2013).

16. Fonfach, J.M., Manderbacka, T., and Neves, M.A.S. "Numerical sloshing simulations: Comparison between Lagrangian and lumped mass models applied to two compartments with mass transfer", *Ocean Engineering*, **114**, pp. 168–184 (2016).

17. Gomez-Gesteira, M., Crespo, A.J.C., Rogers B.D., et al. "Sphysics - development of a free-surface fluid solver- part 2: Efficiency and test cases", *Computers Geosciences*, **48**, pp. 300–307 (2012).

18. Sunara Kusić, M., Radnić, J., Grgić, N., et al. "Sloshing in medium size tanks caused by earthquake studied by SPH", *Gradevinar*, **70**(8), pp. 671–684 (2018).

19. Radnić, J., Grgić, N., Sunara Kusić, M., et al. "Shake table testing of an open rectangular water tank with water sloshing", *Journal of Fluids and Structures*, **81**, pp. 97–115 (2018).

20. Liu, G.R. and Liu, M.B., *Smoothed Particle Hydrodynamics: A Meshfree Particle Method*, World Scientific Publishing Co. Pte. Ltd. (2003).

21. Kelager, M., *Lagrangian Fluid Dynamics Using Smoothed Particle Hydrodynamics*, DIKU, University of Copenhagen (2006).

22. Lucy, L.B. "A numerical approach to the testing of the fission hypothesis", *Astronomical Journal*, **82**, pp. 1013–1024 (1977).

23. Gingold, R.A. and Monaghan, J.J. "Smoothed particle hydrodynamics: theory and application to non-spherical stars", *Monthly Notices of the Royal Astronomical Society*, **181**, pp. 375–389 (1977).

24. Monaghan, J.J. "Smoothed particle hydrodynamics", *Annual Review of Astronomy and Astrophysics*, **30**, pp. 543–574 (1992).

25. Monaghan, J.J. "Smoothed particle hydrodynamics", *Reports on Progress in Physics*, **B**, pp. 1703–1759 (2005).

26. Colagrossi, A. and Landrini, M. "Numerical simulation of interfacial flows by smoothed particle hydrodynamics", *Journal of Computational Physics*, **191**, pp. 448–475 (2003).

27. Monaghan, J.J. "On the problem of penetration in particle methods", *Journal of Computational Physics*, **82**, pp. 1–15 (1989).

28. Crespo, A.J.C., Gómez-Gesteira M., and Dalrymple, R.A. "Boundary conditions generated by dynamic particles in SPH methods", *Computers, Materials, & Continua*, **5**(3), pp. 173–184 (2007).

29. Mahdavi, A. and Talebbeydokhti N. "A hybrid solid boundary treatment algorithm for smoothed particle hydrodynamics", *Scientia Iranica, A.*, **22**(4), pp. 1457–1469 (2015).

30. Sabahi, H. and Nikseresht A.H. "Comparison of ISPH and WCSPH methods to solve fluid-structure interaction problems", *Scientia Iranica, B.*, **23**(6), pp. 2595–2605 (2016).

31. https://wiki.manchester.ac.uk/sphysics/index.php/Main-Page

32. Ordoubadi, M., Yaghoubi, M., and Yeganehdoust, F. "Surface tension simulation of free surface flows using smoothed particle hydrodynamics", *Scientia Iranica*, **24**(4), pp. 2019–2033 (2017).

33. Crespo, A.J.C. "Application of the smoothed particle hydrodynamics model SPHysics to free-surface hydrodynamics", PhD Thesis, Universidade de Vigo, Portugal (2008).

34. Gómez-Gesteira, M., Rogers, B.D., Dalrymple, R.A., et al. "State-of-the-art of classical SPH for free-surface flows", *Journal of Hydraulic Research*, **48**, pp. 6–27 (2010).

35. Para View, Online: www.kitware.com; www.paraview.org

36. Petrov, A.A. and Moiseev, N.N., *Numerical Methods of Calculating the Natural Frequencies of Vibrations of a Bounded Volume of Fluid*, Computing Center of Academy of Sciences of the USSR, Moscow (1966) (in Russian).

37. Newton, R.E., *Finite Element Study of Shock Induced Cavitation*, ACSE Spring Convention, Portland Oregon, April (1980).

38. Brzović, D., Šunjić, G., Radnić J., et al. "Numerical model for fluid-structure coupled problems under seismic load", *Materials with Complex Behaviour II, Advanced Structured Materials*, A. Öchsner et al., Eds. Springer in Germany, **16**, pp. 175–198 (2012).

## Biographies

**Marina Sunara** was born in Croatia, 1986. She obtained her PhD in the field of Structural Engineering, 2017. She has published 25 research and

professional papers in journals and proceedings. Her primary field of interest is numerical and experimental modeling of interaction between fluid and structure. Dr. Sunara has 10 years of teaching experience in various subjects of structural engineering. Currently, she is an Assistant Professor at University of Split, Faculty of Civil Engineering, Architecture and Geodesy.

**Blaž Gotovac** was born in Croatia, 1952. He obtained his PhD in the field of Structural Engineering, 1986. He has published over 80 works: books, book chapters, and research and professional papers in journals and proceedings. His primary field of interest is numerical and experimental modeling of masonry and historical structures. Professor Gotovac has over 40 years of teaching experience in various subjects of structural engineering. Currently, he is a Full Professor at University of Split, Faculty of Civil Engineering, Architecture and Geodesy.

**Jure Radnić** was born in Croatia, 1952. He obtained his PhD in the field of Structural Engineering, 1987. He

has published over 400 works: books, book chapters, and research and professional papers in journals and proceedings. His primary field of interest is numerical and experimental modeling of concrete, masonry and historical structures, as well as interaction between fluid and structure. Professor Radnić has over 40 years of teaching experience in various subjects of structural engineering. Currently, he is a Full Professor at University of Split, Faculty of Civil Engineering, Architecture and Geodesy.

**Alen Harapin** was born in Croatia, 1966. He obtained his PhD in the field of Structural Engineering, 2000. He has published over 150 works: books, book chapters, and research and professional papers in journals and proceedings. His primary field of interest is numerical and experimental modeling of concrete structures, as well as interaction between fluid and structure. Professor Harapin has 30 years of teaching experience in various subjects of structural engineering. Currently, he is a Full Professor and Vicedean at University of Split, Faculty of Civil Engineering, Architecture and Geodesy.